

DeGroot-based opinion formation under a global steering mechanism

Ivan Conjeaud*[◇] Philipp Lorenz-Spreen⁺ Argyris Kalogeratos*[†]

*Centre Borelli, ENS Paris-Saclay, Gif-sur-Yvette, France

[◇]Paris School of Economics, Paris, France

⁺Max Planck Institute for Human Development, Berlin, Germany

[†]Corresponding author: Argyris Kalogeratos

email: argyris.kalogeratos@ens-paris-saclay.fr

Abstract

In this paper we investigate how interacting agents arrive to a consensus or a polarized state. More specifically, we study the opinion formation process under the effect of a global steering mechanism (GSM). We consider that the GSM aggregates agents' opinions at the network level and feeds back to them a form of global information. We propose the *GSM-DeGroot* model, a new two-layer agent-based opinion formation model that captures the coupled dynamics between agent-to-agent local interactions and the GSM's steering effect. This way, agents are subject to the effects of a DeGroot-like local opinion propagation, as well as to a wide variety of possible aggregated information that can affect their opinions, such as trending news feeds, press coverage, polls, elections, etc. The cornerstone feature of our model that, contrary to the standard DeGroot model, allows polarization to emerge, is the differential way in which agents react to the global information. We explore numerically the model dynamics to find regimes of qualitatively different behavior, using simulations on synthetic data. Moreover, we challenge our model by fitting it to the dynamics of real topics, related to protests, social movements, and the escalation of a long geopolitical conflict to a war, which attracted the public attention and were recorded on Twitter. Our experiments show that the proposed model holds explanatory power, as it evidently captures real opinion formation dynamics via a relatively small set of interpretable parameters.

Keywords: Opinion formation dynamics, agent-based modeling, DeGroot model, polarization, global steering, influence of public opinion, information aggregation, media, social networks, mass-movements.

Significance statement: For public debate and opinion formation taking place in a modern landscape of rapid multi-way information exchange, it is of imperative importance to improve our understanding for phenomena such as the emergence of consensus or persistent diversity that leads to polarization and potential conflicts. In this work we present a new two-level opinion formation model. Our model builds upon a DeGroot-based local opinion propagation mechanism with continuous variables for agents' opinions. On the top of that, it considers a global aggregation mechanism that aggregates the agents' opinion-dependent stochastic states that represent publicly visible actions or political participation. This global information is fed back to the agents and functions as a form of global steering, to which, however, the agents are allowed to have differential reactions. Rather than seeking for explanations about consensus and polarization at the level of local contacts, we argue that opinion divergence may more significantly driven by higher level interaction, between agents and aggregated information depicting the state of the whole network. We analyze theoretically our model and highlight various of its properties. Moreover, we use simulations on synthetic data and real data from Twitter to showcase the model's validity, value, and interpretation power to provide insights about complex phenomena through a relatively small number of parameters.

1 Introduction

The explosive development of new electronic communication means is heavily impacting the self-organized social dynamics of opinion formation and political participation, in ways that are not fully-understood. Our limited view over the incurred changes is partly due to the fact that we lack expressive yet interpretable models that could account for the complex multilevel information pathways that become available through modern communication technology. To advance our understanding, what is mostly needed is rather simple models able to highlight a meaningful prototypical agent-based mechanism that drives opinion formation.

The landscape in which modern public debate takes place, includes national and international broadcasting media, and more recently online social networking platforms, which have altered the way and the speed with which people exchange information [1, 2]. Especially for the exchanges on online platforms, these have substituted part of the physical interactions between individuals, and have led to a reshaping of the social network formed around each individual [3], e.g. by having a wider set of contacts including weak-ties and contacts that are geographically remote. The transition from one-to-many to many-to-many communication that these platforms allow has brought new attention to self-organized social behavior, like the new ways of political participation through digital media [4]. Among the interesting related phenomena, one can find some that are emergent, such as price formation, panic buying, overnight formation of social movements, persistent rumors, and self-organized fake news circulation [5, 6, 7, 8]. A recent spur in modeling efforts for such phenomena from a complex system perspective, largely concerns opinion dynamics [9]. Several recent analyses and models have either focused on misinformation spreading or polarization dynamics [10, 11]. Only few modeling efforts have explicitly studied the interplay between individual opinion dynamics, driven locally by social influence, and influenced globally by broadcasting on publicly visible action [12].

At the core of many of the opinion formation studies is the DeGroot-based modeling [13, 14], which basically considers only local interactions between neighboring agents. An agent can still be influenced by any other if there exists a path connecting them, but only through step-by-step bilateral interactions involving intermediaries. Essentially, this simulates the primordial idea that agent's opinion is driven mainly by locally influential individuals [15] and her tendency to conform with her social environment. However, this lacks any mechanism of broadcasting or aggregation of agents' opinions over a matter, or ways for agents to get feedback from the global state of the debate over the network; hence it leaves mass-media effects completely out of its scope. In reality, such mechanisms become more and more relevant due to the fact that its natural for agents who operate under cognitive and time constraints to seek for summarized or filtered information sources. In the modern landscape there are new interacting entities and information pathways [16, 17, 18, 19], as well as the increased coupling of local and global information flows (e.g. mass media picking up on social media trends), which are usually in place simultaneously [20].

Another important source of criticism to the DeGroot-based modeling is its inadequacy for explaining multimodal consensus, also termed as polarization, that is observed increasingly in real-life. Indeed, as agents' opinions get more and more alike to each other, the outcome is for all to converge to a global consensus. As we explain in the next section, existing DeGroot model variations achieve to model polarization only up to a limited extent.

In this paper, we present an extension of the classical DeGroot model that consists of two mechanisms representing two forces that are potentially contradicting: i) a local opinion propagation mechanism that is a *converging* force acting locally and making agents more and more alike, and ii) a global steering mechanism that is a *polarizing* force acting at the global level, which makes agents moving apart from each other. By both performing extensive numerical simulations and mathematically deriving properties we show how the interaction of these two mechanisms allow richer and more complex dynamics, such as disagreement, polarization, and radicalization. We show that there are areas of distinct behavior in different regions of the

model’s parameter space, and that the model offers interpretable descriptions of the associated dynamics. Most importantly, we show that our model is capable of fitting to the approximate dynamics of several phenomena of recent collective movement or action. We also use Twitter data from different linguistic areas, concerning each time the same subject of debate, in order to fit our model and highlight its relevance. The model parameters allow us to interpret and compare such events, and get insights about their characteristics.

The organization of the rest of the paper is as follows. Sec. 2 puts our contribution in perspective to the related work. In Sec. 3.1 we present formally the proposed model and its interpretation. Then, in Sec. 4 we investigate its properties by deriving some of its mathematical properties and exploring its dynamics through an experimental study. In Sec. 5, we fit our model using Twitter data and highlight its interpretability. Finally, we give our conclusions in Sec. 6.

2 Related work

The literature on opinion dynamics mainly comprises two streams, one with models considering opinions as continuous variables, and another one considering them as binary or discrete variables. The first one contains models based on the DeGroot model [13], which is itself a generalization of French’s seminal work [21]. A great variety of generalizations and variations of this model have been proposed, mainly by relaxing the assumption that the influence between any two agents is fixed, and allowing instead to vary as functions of time or the opinion of the nodes [22, 23, 24]. Continuous modeling is not restricted to use DeGroot-Friedkin models [13, 14, 25] as a basis, but rather includes a variety of other models [9, 10, 26, 27]. The other stream of research, initiated by Granovetter [28], considers opinions as binary (or discrete) variables and frequently adopts a game theoretical approach, in which opinions are considered as strategies that give each time the best response to the state of the local environment [29], or a physics-like approach in which opinions are states, with models adapted from physics to social sciences [30, 31]. Often, these models can be summed up to threshold models, where an opinion state is adopted when a sufficiently large proportion of a node’s neighborhood has done so [32]. Both these research streams have boosted the interest in understanding the opinion formation process, consensus formation [13, 33], maintenance of diversity despite increasing local resemblance [34], with some attempts to model global interaction on top of the one at local-level [35, 36]. However, such models are limited by the fact that they consider global interactions that rely on the same peer-to-peer interaction mechanism: nodes interact with their immediate neighbors and sometimes also with others that are arbitrarily distant.

All such models conceptualize the opinion as an internal variable for the agent, and the opinion formation as a process that rarely considers political participation as an important aspect of it. Political participation has been found to be reliably associated with media usage, and especially social media [37, 38]. For an agent, public expression beyond the narrow social environment and political participation are in constant inter-relation with her opinion, which is a mostly overlooked feature of opinion formation.

Despite the fact that the standard DeGroot-based modeling is prototypical and insightful as a basic mechanism, however, as we mentioned in the introduction, it only features a converging mechanism that brings agents more and more opinion-wise closer. The consequence is that, in its basic form, this principle is unable to generate opinion diversity or polarization on its own. To fill the gap, there have been conjectures and speculations about the mechanism that could allow such phenomena to emerge. One idea is that polarization can come from stubborn agents that keep their positions regardless the changes in their social surrounding, and therefore may act as diverse attractors [27, 39]. Another one, also at the local level, stipulates that signed networks that model local disagreement, can also lead to divergence of opinions [40].

To put our work in perspective, in this paper we argue that the diversity generated by the attraction or

repulsion to information aggregation is more important for several reasons, to mention a few: i) a local reaction that would go against the opinion of an agent’s surrounding is likely to be socially costly; ii) this kind of frictional, local, disagreement can be considered negligible compared to the interaction with global information; iii) information aggregation is supposed to be more representative for the state of the debate at the whole network level, and therefore is likely to generate structured reactions, while local disagreement is not. Important to note, though, that our view for divergence at a large-scale is perfectly compatible with ideas of local diversity such as stubborn agents or signed connections between agents, and can therefore be used in combination.

The new opinion formation model we propose aims to capture the intertwined relationship between agent’s opinion, which is a continuous variable, and the publicly visible political expression or participation (e.g. protest participation, posting on social networking platforms, etc), which is a stochastic binary state depending on agent’s opinion. It thereby can be seen as a hybrid model combining elements from both the streams of research at the beginning of the section. A global steering mechanism computes a summary of these states and feeds it back to the agents, who are allowed to have differential reaction to it. This approach overcomes the limitations of standard DeGroot-based models by accounting for information aggregation phenomena. The underlying idea for summarizing the agents’ stated is that peer-to-peer interaction is based on repeated social interaction allowing for more nuance than the steering mechanism, which relies on aggregated coarse information from the whole network.

3 The enhanced GSM-DeGroot model

3.1 Model statement

GSM-DeGroot: Enhanced DeGroot modeling with a global steering mechanism

Let N agents be represented as nodes in a fixed, weighted, directed graph $G = (V, w)$, where $V = \{1, \dots, N\}$ is the set of node indexes, and $w = \{w_{ji}\}_{i,j \in V}$ is a matrix with fixed elements where w_{ji} indicates the influence level of agent j to i . The weights are normalized: $\forall i \in V, \sum_{j=1}^n w_{ji} = 1$.

Each agent i is characterized by: a time-dependent opinion $X_{i,t} \in \mathbb{R}$, which is exchanged locally with neighboring agents through an opinion propagation mechanism (OPM); an opinion-dependent stochastic state $S_{i,t} \in \{0, 1\}$ indicating whether or not the agent manifests her views beyond her local environment ($S_{i,t} = 1$ in the first case), a fixed inherent way $\beta_i \in \mathcal{B} \subseteq \mathbb{R}$ in which she updates her opinion in response to any received global information, where \mathcal{B} is a range of real values around 0. Moreover, we consider $g(S_t)$ to be a function representing the global steering mechanism (GSM) that aggregates information from the network at a global level and feeds it back to the agents as the measured public opinion.

Given the current opinion $X_{i,t}$, the discrete-time evolution of i ’s state and opinion for time $t + 1$ is governed by the two following update rules:

$$\text{State update: } S_{i,t} \sim \text{Bernoulli}\left(\frac{1}{1 + \exp(-\lambda X_{i,t})}\right) \quad (1)$$

$$\text{Opinion update: } X_{i,t+1} = \underbrace{\beta_i}_{\text{agent's reaction}} \underbrace{g(S_t)}_{\text{global steering}} + \underbrace{\sum_{j=1}^N w_{ji} X_{j,t}}_{\text{local opinion propagation}} \quad (2)$$

Therefore, according to Eq. 1, $\mathbb{P}(S_{i,t} = 1) = \frac{1}{1 + \exp(-\lambda X_{i,t})}$ and $\mathbb{P}(S_{i,t} = 0) = 1 - \mathbb{P}(S_{i,t} = 1)$, with λ being

is a sensitivity parameter. For the rest of the presentation, we consider $g(S_t) = \gamma \tilde{S}_t$, where \tilde{S}_t is the number of agents in state 1 at time t , and γ is a parameter expressing the GSM's scaling effect. We call the value of the $g(S_t)$ term as the GSM's *steering strength* at time t .

Note that neutralizing the GSM, by setting $\gamma = 0$, leaves only the OPM in effect, and it becomes equivalent to the classical DeGroot model. Fig. 1 shows schematically the elements of the proposed model.

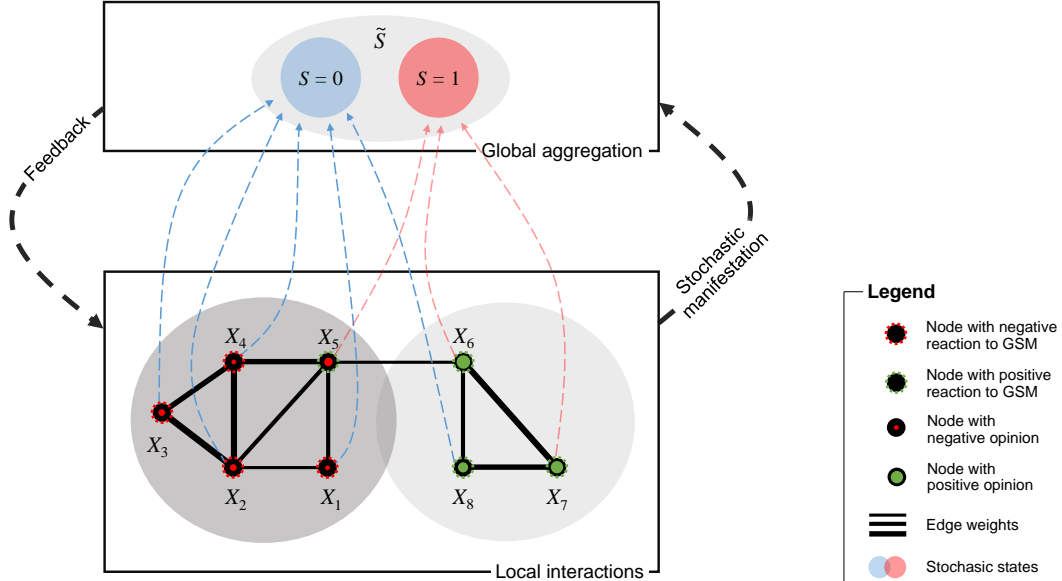


Figure 1: Scheme of the proposed two-layer model. At the bottom there is the *local interaction layer*, and at the top the *global information aggregation layer*. We are at time t (here omitted in the notations). The model assumes that opinions, here X_1, \dots, X_8 (their value scale is shown as red or blue areas inside the nodes), are exchanged at the local level between connected agents through the opinion propagation mechanism (OPM). Then each agent i enters stochastically a state $S_i = \{0, 1\}$ depending on her opinion X_i . Next, the network state is aggregated at a global level, here by counting the number of agents being in state 1 (i.e. \tilde{S}), and finally the global steering mechanism (GSM) feeds back a view over this information that will affect agents' opinion in the next iteration. Each agent reacts to global information in a fixed way, positive or negative (this is β_i , which is shown as dashed green or red node boundaries).

3.2 Interpretation

According to the GSM-DeGroot model, at time t , each agent i is fully described by her set of edge weights $\{w_{ji}\}_{j \in V}$, her opinion $X_{i,t}$, a stochastic state $S_{i,t}$, and her fixed stance over any received global information β_i . The last two elements are additions to the classical DeGroot model [13] and are explained next.

Opinion-dependent states

The state of agent i is stochastically generated each time t by a function that is increasing to her current opinion value $X_{i,t}$, and *independently of her previous state*. Not to be confused with state-based models, here the GSM-DeGroot model is a particular discrete-time stochastic process with variable probability intensity over time (i.e. non-iid events), which is seeded and driven by the opinions. More generally, an agent's state might be regarded as any kind of behavior or action induced by the agent's opinion. For instance, an opinion on the government's policy can lead to protesting against it. A non-deterministic state means that such a decision is taken considering a number of additional factors that are external to the model, which are here assumed to be randomly distributed. For example, deciding whether to participate in a protest is indeed a

function of an agent’s view on the seriousness of a situation, but also a function of her location or allocation of personal time, for which we assume to have no description in the model. Instead, our model uses the parameter λ to describe how much her opinion influences her behavior. For simplicity, here we assume that this mechanism is homogeneous across the population, hence there is a global λ value for all agents.

Steering mechanism and agents’ reaction

Contrary to what the classical DeGroot model assumes, our model formalizes the idea that an agent’s opinion is not only affected by her local social interactions, but also by the global network state. The GSM represents any form of information aggregation that may modify agents’ opinions or perception over a topic of public debate. The GSM is characterized by $\beta \in [0, 1]$, which gives the proportion of positively-reacting agents in the whole population, and the function g , which, in the simple form introduced below Eq. 2, is described by the parameter γ .

4 Results

4.1 Distinct properties of the opinion propagation and steering mechanisms

Our model comprises two intertwined mechanisms (Fig. 1) that are incorporated formally in the update rule of Eq. 2. The second term corresponds to the effect of the OPM on agent i through direct social influence along the graph edges. The first term corresponds to the effect of the GSM, subject to the agent’s reaction to it (β_i). Next, we discuss the distinct properties of the two mechanisms when considered separately. We establish that, each mechanism exhibits stereotypical behavior that informs us on its nature and role: the OPM acts as a “*converging force*”, whereas the GSM acts as a “*polarizing force*”.

Opinion propagation mechanism (OPM)

As mentioned in Sec. 3.1, taken separately (i.e. $\gamma = 0$), the OPM is exactly the *DeGroot opinion update rule*: for agent i at time t , this is $X_{i,t+1} = \sum_{j=1}^N w_{ji} X_{j,t}$. Consequently, the OPM acts like a smoothing operator that makes the opinions more and more similar. In fact, the DeGroot model has a notable inherent property that, under weak assumptions, *consensus* is always reached [13]. Formally:

Definition 1. – Consensus. *The system reaches consensus when the opinions of all agents converge to the same finite value:*

$$\exists C \text{ s.t. } \forall i \in V, \lim_{+\infty} \mathbb{E}[X_{i,t}] = C. \quad (3)$$

It can be easily shown that consensus induces the following property (see proof in Appendix A).

Proposition 1. – Narrowing behavior over time. *Under the weak assumption of normalized incoming edge weights for all nodes, one can prove that for all $i \in V$: $\min_i \{X_{i,t}\}$ is an increasing sequence, and $\max_i \{X_{i,t}\}$ is a decreasing sequence over time.*

Therefore, not only is it impossible for the DeGroot model to converge to a polarized state, but also it monotonically reduces the maximal diversity of the system, since the two most “extreme” opinions can only get closer to each other as time passes. Note, however, that this does not hold in the case of signed networks, as [40] illustrates; a related discussion is provided in the Appendix C.

Global steering mechanism (GSM)

Let us consider the special case of the GSM-DeGroot model (Sec. 3.1) where only the GSM is in effect, i.e. $\forall i, j \in V$ with $j \neq i, w_{ji} = 0, w_{ii} = 1$. At each time $t + 1$ the opinion update rule for agent i reduces to:

$$X_{i,t+1} = \beta_i g(S_t) + X_{i,t}. \quad (4)$$

Proposition 2. – Two diverging groups. If $\beta^+ = \{i \in V : \beta_i = 1\} \neq \emptyset$, and $\beta^- = V \setminus \beta^+$ its complementary, the two sets with opposite reaction to global information, then:

$$\lim_{+\infty} \mathbb{E}[X_{i,t}] = \begin{cases} +\infty & i \in \beta^+; \\ -\infty & i \in \beta^-. \end{cases} \quad (5)$$

Therefore, in the absence of local interactions, the two groups of agents, reacting oppositely to global information, will get farther and farther away from each other over time. The proof is provided in Appendix A.

4.2 Interplay between the opinion propagation and steering mechanisms

In Sec. 4.1, we considered GSM and OPM separately. Here, we are interested in the interplay between those two mechanisms, and the implication on the GSM-DeGroot dynamics. Let us first mention some quantities that will be used later. First, μ is the mean initial opinion that gives the magnitude of the initial shock; in practice, we will be drawing the initial opinions from Normal distribution centered around zero. Moreover, for time t , let the average opinion be \bar{X}_t , and the maximum opinion diversity between any pair of agents be:

$$D_{\max,t} = \max_{i \in V}(X_{i,t}) - \min_{j \in V}(X_{j,t}). \quad (6)$$

Similarly, we can speak about the final outcome at $t \rightarrow +\infty$ (in practice, at some long enough time-horizon) as $D_{\max,\infty} = \max_{i \in V}(C_i) - \min_{j \in V}(C_j)$, where C_i is i 's converging opinion (see Definition 1), or the overall maximal diversity throughout the process $D_{\max} = \max_t D_{\max,t}$. Note that $D_{\max,t}$ (or D_{\max}) can also be seen as an upper-bound for polarization.

From the opinion update rule of Eq. 2, we can derive the following interesting relation between the average opinions at two subsequent time steps:

$$\bar{X}_{t+1} = (\sum_{i \in V} \beta_i) g(S_t) + \bar{X}_t. \quad (7)$$

For the sake of simplicity, we will use $g(S_t) = \gamma \tilde{S}_t$ (see Sec. 3.1), and agent reactions to GSM $\beta_i \in \{-1, 1\}, \forall i \in V$. Let also the ratio of agents reacting positively be $\beta = \frac{1}{N} \sum_{i \in V} \mathbf{1}\{\beta_i = 1\}$. Thus Eq. 7 now boils down to:

$$\bar{X}_{t+1} = (2\beta - 1)\gamma \tilde{S}_t + \bar{X}_t. \quad (8)$$

Qualitatively, this identifies two different regimes:

- **self-cooling** for $\beta < \frac{1}{2}$: the average opinion decreases; any additional agent entering state 1 yields a negative effect for the majority of agents, thus reducing further the probability for the majority to enter in state 1.
- **self-exciting** for $\beta > \frac{1}{2}$: the average opinion increases; any additional agent entering state 1 yields a positive effect for a majority of agents, thus increasing further the probability for the majority to enter in state 1.

In Appendix C, we show the results of simulations illustrating the implication of this on the dynamics of extreme opinions.

Effects on maximal polarization

While the OPM works against allowing the GSM to drive the two groups in two opposite directions, the latter *always* prevents the former from making agents alike to the point that they reach consensus. The technical results in the two following propositions illustrate this specific role of the GSM.

Proposition 3. – No consensus under GSM. *If the GSM is in effect (if $\gamma > 0$), consensus is impossible to be reached.*

Definition 2. – ε -consensus. *If $\forall i \in V, \exists C_i$ s.t. $\lim_{+\infty} \mathbb{E}[X_{i,t}] = C_i$, then all opinions have converged to some finite values, and we say that we have an ε -consensus iff: $D_{\max, \infty} = \max_{i \in V}(C_i) - \min_{j \in V}(C_j) \leq \varepsilon$.*

Proposition 4. – Boundary on ε -consensus. *For a strictly increasing $g(S_t)$ function, reaching a $(\lim_{+\infty} \mathbb{E}[g(S_t)])$ -consensus is not possible. For the special GSM form of $g(S_t) = \gamma \tilde{S}_t$, this corresponds to a $(\gamma \lim_{+\infty} \mathbb{E}[\tilde{S}_t])$ -consensus.*

The first result is trivial to interpret: the GSM always prevents consensus, whereas the OPM alone would yield consensus (under weak assumptions). The second one implies that when each agent converges to her fixed -but not necessarily the same- C_i value, extreme opinions cannot get closer than what the GSM strength allows. In other words, the stronger the steering is, the stronger will be the difference between the extremes at the end, too. Although this is true in the limit and in the case of individual convergence to fixed values, yet it provides insight to the GSM’s role.

Self-cooling, self-excitation: effects on final polarization

To investigate further, we use Barabasi-Albert graphs (with 100 nodes) to simulate our model, and we provide two kinds of heatmaps in Fig. 2 illustrating the metrics of maximal polarization D_{\max} and final polarization $D_{\max, \infty}$ as a function of γ and μ (indirectly controlling the initial GSM steering strength). On top of interacting with the OPM, the GSM interacts *with itself* in the sense that in $g(S_t) = \gamma \tilde{S}_t$, \tilde{S}_t clearly depends on previous values $\{\gamma \tilde{S}_{t'}\}_{t' < t}$. In the self-cooling regime, higher values of previous steering strength tend to decrease \tilde{S}_t , whereas in the self-exciting regime, it’s the opposite.

This essentially explains the difference observed between the two regimes when looking at the final polarization level. First, note that the values of the polarization metrics are way lower in the first case (the steering strength vanishes over time). In the self-exciting case, a higher steering strength induces a larger final polarization, as expected. When it comes to the self-cooling, we observe the opposite: increasing μ and γ leads to a polarization decrease. This is due to the fact we pointed out earlier: increasing μ and γ , yields higher steering strength in the early steps, which leads to further reduction of polarization in the next ones. This interpretation is supported by the behavior of the D_{\max} metric, which has similar variation in both cases. Thus, in the self-cooling regime, the maximal polarization is higher for higher strength of the steering mechanism, causing a polarization reduction later and at the end of the trial.

Effect of selected parameters on the number of agents in state 1

In the following, we simulate our model using networks generated by the Stochastic Block Model (SBM) [41] (details are given in Appendix C). The synthetic graph has 100 nodes, comprising two communities of 70 and 30 nodes, and proportion of agents with positive reaction to information respectively 0.3 and 0.7. In SBM, a parameter r controls the probability for two agents from different communities (clusters) to be connected, thus a higher value indicates a more well-clustered networks. We specifically look at the effects of three important parameters with interpretative power, μ , γ , r , on the number of agents in state 1, i.e. $\tilde{S}_t = \sum_{i \in V} \mathbf{1}\{S_{i,t} = 1\}$. The simulation results are presented in Fig. 3.

The effect of μ is two-fold. It controls the probability for agents to initially be in state 1, and thus gives the departure point of the curves, but by so doing it also ignites the GSM. As a consequence, the peak of the curve as well as the time at which it is reached depend on it: the lower μ , the longer it takes for the GSM to amplify the initial situation and the weaker it is, thus the lower the peak. Concerning γ , one can see that it controls also the height of the peak (the higher γ , the stronger the steering, and hence, the higher the peak) as well as for the time at which the curve peaks: the higher γ , the longer it takes for the peak to be reached. It also seems that γ has an effect on the decrease after the peak, as high values of γ associate to quicker decrease. This can be interpreted as the decrease being sharper when the GSM is stronger (since we are in

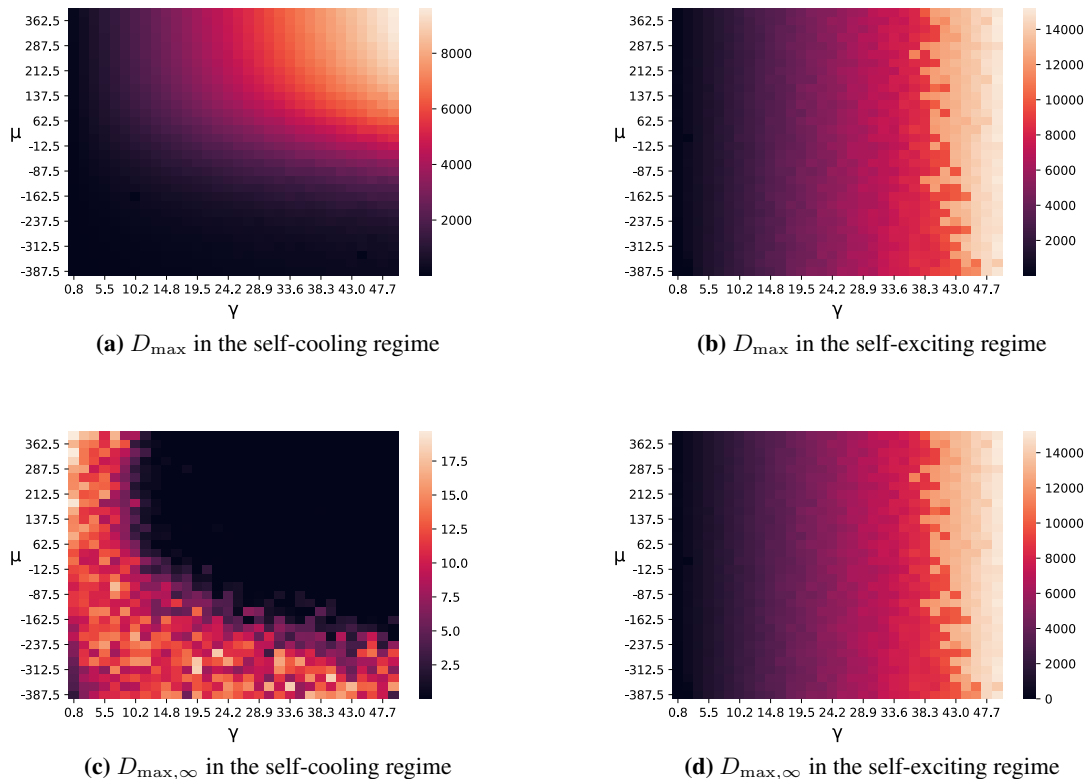


Figure 2: Effect of μ (controls the initial number of agents in state 1) and γ (GSM’s scaling parameter) on two polarization metrics: the maximal polarization D_{\max} and the final polarization $D_{\max,\infty}$. We show one instance in the self-cooling ($\beta = 0.05$) regime, and one instance in the self-exciting ($\beta = 0.95$) regime.

the self-cooling case). Finally, since r controls the inter-community connectivity, it hence affects mainly the speed in which the model “cools down”. In this specific setting, r reduces the effect of the GSM as it mixes the minor community (positively reacting) with the major one (negatively reacting).

5 Confrontation with real-world data

In this section, we aim to assess the capacity of the GSM-DeGroot model in practice, by fitting its parameters in order to capture the dynamics of real-world data. Our goal is not necessarily to achieve the best possible fit, but rather to offer a quantitative interpretation of the phenomena appearing in real situations.

Dealing with online social network data

Acquiring access to data concerning the exact connectivity of a physical or online social network, or the actual opinions of individuals over a subject, is very hard. However, the architecture of the GSM-DeGroot model allows us to consider opinions as latent variables, and then to use the agents’ states (the S_i ’s) as observed behaviors generated by those underlying opinions. We use Twitter data from StoryWrangler [42]¹, and specifically data concerning the frequency of use of specific characteristic *terms*, namely hashtags or symbols, in the tweets written in a certain language. We thereby interpret the use of such a term by the i -th

¹Online tool: <https://storywrangling.org/>

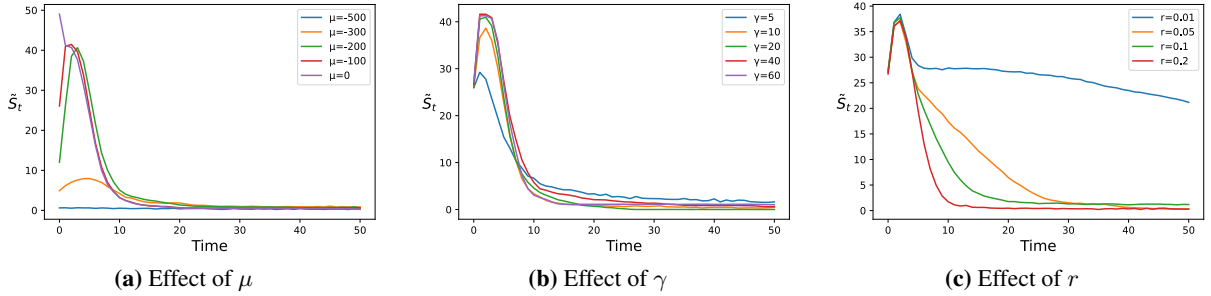


Figure 3: Effect of μ (controls the initial number of agents in state 1), γ (GSM’s scaling parameter), and r (controls the inter-community connectivity) on the number of agents in state 1, i.e. \tilde{S}_t .

agent as a publicly visible behavior, manifesting her state S_i . In each scenario, we focus on a single term.

Here we focus on three use-cases: the *Black Lives Matter* (BLM) and the *MeToo* movements, as well as the geopolitical conflict and the subsequent military invasion of Ukraine by Russia in February 2022. The respectively terms we picked as representatives are the #BlackLivesMatter (though denoted in the rest as #BLM), #MeToo, and the emoji of the Ukrainian flag. The choice of those topics is motivated by two facts: i) they have had world-wide attention, which allows for comparison between diverse countries; ii) they fit with the timeline considered in our model: an initial triggering event ² triggers both a collective process of debate and protests, and wide media coverage. As objective, we desire to fit our model with data concerning several languages, and then compare the outcomes.

Fitting GSM-DeGroot to data

As mentioned, we have each time at our disposal the aggregate frequency of use over time of a specific term in the tweets issued in a given language. It is very important to clarify once again that we have no way to know the actual interaction network. To overcome this limitation, we generate a the graph of a *synthetic twin network* in each case that, although small and rather prototypical, we believe it can still be used for studying which values of the model parameters best reproduce real recorded behaviors. We assume a simple synthetic graph generated by a typical SBM [41]. The graph has two communities, each one having a different composition of agents reacting differently to global information . The choice to consider a two-community structure comes from our intention to model the interaction of (roughly) two adversarial groups of individuals, as it can often be the case in social media³. The degree with which those communities are linked, r , is of primary importance as it measures the degree of clusterability of the synthetic population over the topic we consider. The size of clusters, as well as their compositions in terms of reaction to information were fixed beforehand so as to set ourselves into the self-cooling regime to avoid exploding dynamics (i.e. to have $\beta < \frac{1}{2}$, see Sec. 4.2). Investigating further how to best synthesize a surrogate population is beyond the scope of this work, but could be of interest for future research in order to increase the precision of an empirical study.

The GSM-DeGroot fitting process is as follows: we first generate a synthetic SBM network, and then simulate the model using different parameters. We restrict the model parameter space to a grid for $\{\mu, \gamma, r\}$.

²*BLM*: the event was the murder of George Floyd by police officer Derek Chauvin. The BLM movement was actually initiated years before, after a similar incident that took place in Ferguson. However, here we focus on the second wave of the movement, which was triggered in Minneapolis and went viral worldwide. – *MeToo*: the Jeffrey Epstein case, who took advantage of his position as a Hollywood producer and sexually abused several women. – *Invasion of Ukraine*: the initiation of the “*special military operation*” that was the invasion of Ukraine by Russia on the 24th of February 2022.

³We are aware that this is a simplification. For instance, in 2018 Gaumont, Panahi, and Chavalarias reported five communities in the French Twitter political landscape [43]. However, we argued earlier that we believe that this is sufficient for a demonstration that does not aim to accuracy, but rather highlight the potential of the GSM-DeGroot model.

We use a scale-invariant metric to compare the real time-series of the number of agents in state 1 (i.e. \tilde{S}_t) and the time-series produced by the simulation of our model. The outcome of our optimization process is a set of value triplets (μ^*, γ^*, r^*) , one for each considered language.

Results

The triplet (μ^*, γ^*, r^*) that achieved the best model fitting to the real data for each considered language is reported in a tabular format in Appendix B. For #MeToo, we consider two groups of languages, “European” (E) and “Non-European” (NE)⁴. For #BLM, on the other hand, we look at two categories, namely “West-European” and “Eastern-Central European” languages⁵. Concerning the Ukrainian events, we also plot the results on a map of Europe to identify salient differences between countries and geographical regions.

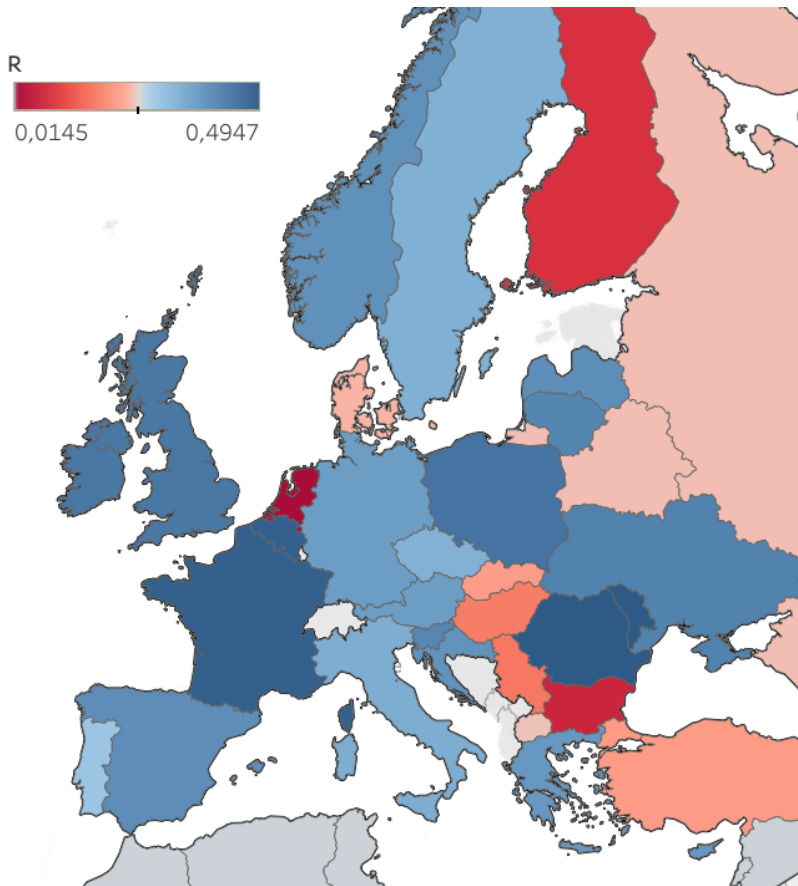


Figure 4: Visualization of the country-wise estimation of the r^* over a map of Europe.

Looking at the mean values of the outcome parameters for each language category allows us to broadly compare the phenomena taking place in those linguistic-geographical areas. When it comes to #MeToo (see Appendix B Tab. 1), the centroid of the category “European” language is $\{\mu_E^* = -98.423, \gamma_E^* = 19.423, r_E^* = 0.161\}$, whereas the one of “Non-European” languages is $\{\mu_{NE}^* = -112.824, \gamma_{NE}^* = 14.485, r_{NE}^* = 0.234\}$. So we can note that $\mu_E^* > \mu_{NE}^*$, which can be interpreted as the informational shock being larger for European languages. This would correspond to the Weinstein case having initially more impact in Europe and America than elsewhere. Also, $\gamma_E^* > \gamma_{NE}^*$, which corresponds to a more influential global steering mechanism (GSM), and thus can be interpreted as the fact that higher media attention was given to the #MeToo movement in

⁴Of course, “Non-European” is not a meaningful category *per se*; our aim here is simply to highlight a Europe and America’s specificity concerning the topic, not to pin down a “non-European” specificity.

⁵Admittedly, this uses is rule of thumb and may not correspond to the best grouping.

Europe and America compared to other places. However, it is important to note that because of the use of a scale-invariant distance, it is possible -but not obvious- that those two parameters cannot be interpreted as easily, in particular for #BLM. The parameter in which we are mostly interested, since it is probably not affected by the scaling-invariance, is r that controls how clustered the network is (see Sec. 4.2). In simple terms, r represents how clustered the synthetic network is, and in particular low values of r indicate two distinct groups alighting a controversy, and thus an important polemic subject that through debate can lead to polarization. Therefore, note that $r_{NE}^* > r_E^*$.

Concerning the values for γ^* and μ^* for #BLM (see Appendix B Tab. 2), we note that the differences between language groups are not easy to interpret, and are probably uninformative, which may make one doubt about the interpretation given previously for #MeToo. However, the difference here for r^* is pretty meaningful: this value for Eastern Europe is more than double than the one for Western Europe, which makes sense with the interpretation given to low values of parameter r . This would indicate that in Eastern Europe, the BLM topic has not been really divisive, and thus has not led to much debate and activities or actions.

Fig. 4 shows the outcome of the optimization process for the Ukrainian case, and more associates colors to values of r^* for countries in Europe in which the corresponding language is spoken. Results for all parameters are presented in Tab. 3 in Appendix B. Shades of red indicate the subject being rather polemic in the associated country, whereas shades of blue indicate the opposite. First thing we note is the difference between Ukraine and Russia (and Belarus, considered a Russian speaking country): the results indicate that the topic has been way more consensual in Ukraine than in Russia, which makes sense given the anti-war movement inside Russia⁶. Second, we note the results to be particularly relevant for Finland (due to the historical ties with Russia, its proximity, and its recent application to become a NATO member), Bulgaria (which has undergone a heated debate concerning whether or not Ukraine should be supported), Serbia (historical and religious ties with Russia), Hungary, and Turkey (due to strong ties with Russia and their ambivalent position)⁷. Finally, we note that the topic is more consensual in the UK, France, and Spain compared to Germany, Italy, and Czech Republic, which we interpret as being the effect of those countries' high energetic dependence on Russian gas.

6 Conclusions

In this work we presented the two-layer opinion formation model called GSM-DeGroot. In our approach, each agent is characterized by a continuous opinion variable as well as a binary state accounting for actions or behavior induced stochastically by the agent's opinion. Our model features two distinct mechanisms: the opinion propagation mechanism (OPM) that formally corresponds to the classic DeGroot model and acts as a converging force, and the global steering mechanism (GSM) that aims to model the feedback received by agents concerning information at the network level and acts as a diverging force. By mathematically deriving the properties of those mechanisms and investigating their interplay using numerical simulations, we show that: i) the GSM prevents agents from reaching a consensus and imposes a bound on reachable ε -consensus; ii) the GSM has a differentiated effect on limiting the maximal diversity depending on which of the two identified regimes (self-cooling or self-exciting) does the process lie on. These findings offer a new way to explain how various polarization phenomena can emerge through the differential interactions of agents with global information aggregation.

⁶Note also that probably the debate inside Ukraine is underestimated since the Russian speaking population inside Ukraine rather counts for the result associated to Russia.

⁷The result concerning the Netherlands is surprising and difficult to interpret. This can be due to data quality problems or/and bad model fitting.

In our experimental study, we fit our model to Twitter data concerning the frequency of use of specific symbols and hashtags in tweets (implying agents being at state 1 of our model) written in different languages. We investigated the role of interpretable parameters to show that our model is able to reproduce meaningful differences between geographical regions or countries.

As part of future investigations, there can be interesting refinements of the model, namely to combine it with complementary features, such as different agent roles (e.g. influencers or stubborn agents) and signed networks, or other features such as introducing influence saturation or thresholding. Furthermore, the analysis of real data can be greatly benefited by further improvements to the model fitting procedure.

Acknowledgments

Philipp Lorenz-Spreen acknowledges financial support from the Volkswagen Foundation (grant “Reclaiming individual autonomy and democratic discourse online: How to rebalance human and algorithmic decision making”). Argyris Kalogeratos acknowledges the support from the Industrial Data Analytics and Machine Learning (IdAML) Chair hosted at ENS Paris-Saclay, University Paris-Saclay.

APPENDICES

A Proofs of technical results

In the rest we refer to the following quantities: let the minimum and maximum opinion at time t be denoted by $x_t = \min_i(X_{i,t})$, and $X_t = \max_i(X_{i,t})$ (note that, in this case, x_t and X_t are indexed only by the time).

Importance of the assumption for normalized weights

We suppose the graph is fixed over time, and we consider $\forall i \in V$, $\sum_{j=1}^N w_{ji} = \alpha$, with $\alpha \geq 0$. Then, the magnitude of each opinion in the limit can be:

$$\lim_{+\infty} |X_{i,t}| = \begin{cases} +\infty & \text{when } \alpha > 1; \\ 0 & \text{when } 0 \leq \alpha < 1. \end{cases} \quad (9)$$

Therefore, same as for the DeGroot model, in order for the GSM-DeGroot model to be meaningful and interpretable, it is required to have normalized edge weights induced by $\alpha = 1$.

Proof

At each time t ,

$$\left\{ \begin{array}{l} \text{the update rule for each agent } i \text{ gives} \\ \text{which implies that} \\ \text{and immediate induction yields} \\ \text{the latter, by definition yields } \forall i, \end{array} \right. \begin{array}{l} \alpha x_t \leq X_{i,t+1} \leq \alpha X_t, \\ \alpha x_t \leq x_{t+1} \leq X_{t+1} \leq \alpha X_t, \\ \alpha^t x_0 \leq x_{t+1} \leq X_{t+1} \leq \alpha^t X_0; \\ \alpha^t x_0 \leq X_{i,t+1} \leq \alpha^t X_0. \end{array} \quad (10)$$

And finally, using the last expression (for $X_{i,t}$), the result follows naturally from the following inequality:

$$\alpha^t \min(|x_0|, |X_0|) \leq |X_{i,t}| \leq \alpha^t \max(|x_0|, |X_0|). \quad (11)$$

As a consequence, the assumption for normalized edge weights (i.e. $\alpha = 1$) is needed to ensure that the models are informative and interpretable.

Proposition 1. *Under the weak assumption of normalized incoming edge weights for all nodes, one can prove that for all $i \in V$: x_t is an increasing sequence, and X_t is a decreasing sequence over time.*

Proof. The proof relies on the same arguments we used previously. Using normalized edge weights ($\alpha = 1$), the result comes from Eq. 10: $\alpha x_t \leq x_{t+1} \leq X_{t+1} \leq \alpha X_t$. \square

Proposition 2. *In the pure GSM setting, if $\beta^+ = \{i \in V : \beta_i = 1\} \neq \emptyset$, and $\beta^- = V \setminus \beta^+$ its complementary, the two sets with opposite reaction to global information, then:*

$$\lim_{+\infty} \mathbb{E}(X_{i,t}) = \begin{cases} +\infty & i \in \beta^+; \\ -\infty & i \in \beta^-. \end{cases} \quad (12)$$

Proof. Let $i, j \in V : \beta_i = 1, \beta_j = -1$. i 's update rule yields:

$$X_{i,t+1} - X_{i,t} = g(S_t) \geq 0. \quad (13)$$

Thus, $\mathbb{P}(S_{i,t+1} = 1) \geq \mathbb{P}(S_{i,t} = 1)$. Then

$$\mathbb{E}[g(S_t)] > \mathbb{P}(S_t = 1)g(1) \geq \mathbb{P}(S_{i,t} = 1)g(1) \geq \mathbb{P}(S_{i,0} = 1)g(1) > 0, \quad (14)$$

so that $\exists \eta > 0$ s.t. $\forall t, \mathbb{E}[g(S_t)] > \eta$. Taking the expectation of the update rule for i and j gives:

$$\mathbb{E}[X_{i,t}] = \mathbb{E}[X_{i,0}] + \sum_{\tau=0}^{t-1} \mathbb{E}[g(S_t)] \geq \mathbb{E}[X_{i,0}] + \eta t, \quad (15)$$

$$\mathbb{E}[X_{j,t}] = \mathbb{E}[X_{j,0}] + \sum_{\tau=0}^{t-1} \mathbb{E}[g(S_t)] \leq \mathbb{E}[X_{j,0}] - \eta t. \quad (16)$$

The result is obtained by taking the limit in the right-hand side of the inequality. \square

Lemma 1. *Let $g : \{0, 1\}^N \rightarrow \mathbb{R}^+$ be an increasing function in the sum of S_i 's, and such that $g(S_t) = 0 \Leftrightarrow S_t = (0, \dots, 0)$. Then,*

$$\lim_{+\infty} \mathbb{E}[g(S_t)] = 0 \Rightarrow \forall i \in V, \lim_{+\infty} \mathbb{E}(X_{i,t}) = -\infty. \quad (17)$$

Proof. Assume $\lim_{+\infty} \mathbb{E}[g(S_t)] = 0$. For any t , one can write $\mathbb{E}[g(S_t)] = \sum_{k=0}^N \mathbb{P}(S_t = k)g(k)$, so that clearly $\lim_{+\infty} \mathbb{E}[g(S_t)] = 0$ implies $\lim_{+\infty} \mathbb{P}(\tilde{S}_t = 0) = 1$, and thus $\lim_{+\infty} \mathbb{E}(\tilde{S}_t) = \lim_{+\infty} \sum_{k=0}^N \mathbb{P}(\tilde{S}_t = k)k = 0$. However since $\mathbb{E}[\tilde{S}_t] = \mathbb{E}[\sum_{i \in V} S_{i,t}]$, clearly $\lim_{+\infty} \mathbb{E}[\tilde{S}_t] = 0$ implies $\forall i \in V, \lim_{+\infty} \mathbb{E}(S_{i,t}) = 0$, that is

$$\lim_{+\infty} \mathbb{E}\left[\frac{1}{1 + \exp(-\lambda X_{i,t})}\right] = 0. \quad (18)$$

Assume $\exists M, \eta$ such that $\forall t_0, \exists t > t_0$ s.t. $\mathbb{P}(X_{i,t} > M) > \eta$, then, denoting $f_{i,t}$ the density function of $X_{i,t}$,

$$\int_{-\infty}^{+\infty} \frac{1}{1 + \exp(-\lambda x)} f_{i,t}(x) dx = \int_{-\infty}^M \frac{1}{1 + \exp(-\lambda x)} f_{i,t}(x) dx + \int_M^{+\infty} \frac{1}{1 + \exp(-\lambda x)} f_{i,t}(x) dx, \quad (19)$$

so that

$$\mathbb{E}[\tilde{S}_t] \geq \mathbb{E}[S_{i,t}] > \frac{1}{1 + \exp(-\lambda M)} \eta, \quad (20)$$

which contradicts $\lim_{\infty} \mathbb{E}[\tilde{S}_t] = 0$. Thus we conclude $\forall M, \lim_{\infty} \mathbb{P}(X_{i,t} > M) = 0$. Now we need to show that:

$$\forall M, \lim_{\infty} \mathbb{P}(X_{i,t} > M) = 0 \implies \lim_{+\infty} \mathbb{E}[X_{i,t}] = -\infty. \quad (21)$$

Assume $\forall M, \lim_{\infty} \mathbb{P}(X_{i,t} > M) = 0$. Assume $\exists [a, b] \subset [0, +\infty[$ s.t. $\forall t_0, \exists t > t_0, f_{i,t}(x) \geq f_{i,0}(x)$ almost everywhere. Then clearly:

$$\mathbb{P}(X_{i,t} \geq a) \geq \mathbb{P}(b \geq X_{i,t} \geq a) = \int_a^b f_{i,t}(x) dx \geq \int_a^b f_{i,0}(x) dx, \quad (22)$$

which yields a contradiction. Thus $\forall [a, b] \subset [0, +\infty[, \exists t_0$ s.t. $f_{i,t}(x) < f_{i,0}(x)$ almost everywhere. Then clearly. Furthermore, $\forall M, \forall \varepsilon > 0, \exists t_0$ s.t. $\forall t > t_0, \mathbb{P}(X_{i,t} \leq M) \geq 1 - \varepsilon$. Let $M < 0$, one has $\mathbb{E}[X_{i,t}] = \int_{-\infty}^M x f_{i,t}(x) dx + \int_M^0 x f_{i,t}(x) dx + \int_0^{+\infty} x f_{i,t}(x) dx$, and thus:

$$\mathbb{E}[X_{i,t}] \leq M(1 - \varepsilon) + \int_0^{+\infty} x f_{i,0}(x) dx \quad \text{for } t \text{ large enough.} \quad (23)$$

Thus $\forall M < 0, \exists t_0$ s.t. $\forall t > t_0, \mathbb{E}[X_{i,t}] \leq M$, so finally, $\lim_{+\infty} \mathbb{E}[X_{i,t}] = -\infty$. \square

Lemma 2. *If there exists i such that $\forall j \in \mathcal{N}_i \cap \{i\}, \exists C_j / \lim_{+\infty} \mathbb{E}[X_{j,t}] = C_j$, then $\lim_{+\infty} \mathbb{E}[g(S_t)]$ exists and is finite. Proof of this proposition is trivially obtained by manipulating the update rule.*

Lemma 3. For any i , if $\forall i, \exists C_i / \lim_{+\infty} \mathbb{E}[X_{i,t}] = C_i$ one cannot have $\exists C_i \in \mathbb{R}$ s.t. $\forall j \in \mathcal{N}_i \cup \{i\}, \lim_{+\infty} \mathbb{E}[X_{j,t}] = C_i$.

Proof. Suppose there is one i such that $\forall j$ in i 's neighborhood $\lim_{+\infty} \mathbb{E}[X_{j,t}] = C_i$ and $\lim_{+\infty} \mathbb{E}[X_{i,t}] = C_i$. Then the update rule yields:

$$\mathbb{E}[X_{i,t+1}] - \sum_j w_{ji} \mathbb{E}[X_{j,t}] = \beta_i \mathbb{E}[g(S_t)] \quad (24)$$

Lemma 2 allows us to take the limit in the last equation, which yields:

$$C_i - C_i \sum_j w_{ji} = \beta_i \lim_{+\infty} \mathbb{E}[g(S_t)], \quad (25)$$

which, by the normalized-weights assumption, yields:

$$\lim_{+\infty} \mathbb{E}[g(S_t)] = 0, \quad (26)$$

and together with Lemma 1 yields a contradiction. \square

Proposition 3. No consensus is a natural corollary of Lemma 3, by taking $\forall i \in V, C_i = C$.

Proof. No consensus is a natural corollary of Proposition 3, by taking $\forall i \in V, C_i = C$. \square

Lemma 4. Suppose $\forall i \in V, \exists C_i / \lim_{+\infty} \mathbb{E}[X_{i,t}] = C_i$. Then:

$$\lim_{+\infty} \mathbb{E}[X_{i,t}] = \min_{i \in V} (C_i) \Rightarrow \beta_i = -1, \quad (27)$$

and:

$$\lim_{+\infty} \mathbb{E}[X_{i,t}] = \max_{i \in V} (C_i) \Rightarrow \beta_i = 1. \quad (28)$$

Proof. Let $i \in V$ such that $C_i = \min_{i \in V} (C_i)$. Then taking the limit in i 's update rule gives:

$$C_i = \sum_{j \in \mathcal{N}_i} w_{ji} C_j + \beta_i \lim_{+\infty} \mathbb{E}[g(S_t)] \geq C_i + \beta_i \lim_{+\infty} \mathbb{E}[g(S_t)]. \quad (29)$$

We know from Lemma 1 that $\lim_{+\infty} \mathbb{E}[g(S_t)] \neq 0$, so that we must have $\beta_i < 0$ and thus $\beta_i = -1$. The proof for the second part of the proposition is similar. \square

Proposition 4. For a strictly increasing $g(S_t)$ function, reaching a $(\lim_{+\infty} \mathbb{E}[g(S_t)])$ -consensus is not possible. For the special GSM form of $g(S_t) = \gamma \tilde{S}_t$, this corresponds to a $(\gamma \lim_{+\infty} \mathbb{E}[\tilde{S}_t])$ -consensus.

Proof. Suppose we have an ϵ -consensus then clearly:

$$\forall i \in V, C_i \leq \min_{i \in V} (\{C_i\}) + \epsilon. \quad (30)$$

Let $i^* \in V$ such that $C_{i^*} = \min_{i \in V} (\{C_i\})$. From Proposition 4 we know that $\beta_{i^*} = -1$, so that, using the update rule we can write:

$$C_{i^*} \leq C_{i^*} + \epsilon - \lim_{+\infty} \mathbb{E}[g(S_t)], \quad (31)$$

which gives:

$$\lim_{+\infty} \mathbb{E}[g(S_t)] \leq \epsilon. \quad (32)$$

This gives Proposition 4 by contraposition. \square

B Tables of numerical results

Category	Language	Error (\downarrow)	Best parameters			Category average		
			μ^*	γ^*	r^*	$\bar{\mu}$	$\bar{\gamma}$	\bar{r}
European	Swedish	0.251	-150.899	29.573	0.071	-98.423	19.420	0.161
	French	0.331	-97.398	30.275	0.122			
	German	0.361	-87.777	17.574	0.379			
	Portuguese	0.429	-120.259	9.323	0.238			
	Dutch	0.435	-175.000	27.500	0.025			
	English	0.454	-120.219	6.734	0.249			
	Spanish	0.472	-148.704	12.374	0.167			
	Greek	0.472	-110.551	8.951	0.022			
Non European	Catalan	0.588	125.000	32.500	0.175	-112.824	14.485	0.234
	Arabic	0.344	-147.889	15.114	0.256			
	Tamil	0.372	-100.820	20.386	0.061			
	Kannada	0.534	-200.527	10.058	0.032			
	Korea	0.538	-100.593	19.843	0.198			
	Turkish	0.552	-132.869	17.481	0.314			
	Hindi	0.583	-68.538	10.655	0.427			
Persian	0.651	-38.534	7.860	0.350				

Table 1: #MeToo social movement – Results obtained by our optimization process using Twitter data. The best model parameters (μ^*, γ^*, r^*) estimated for each language and the corresponding fitting error are reported. The languages are grouped into geographic categories, within which their order is from lower to higher fitting error.

Category	Language	Error (\downarrow)	Best parameters			Category average		
			μ^*	γ^*	r^*	$\bar{\mu}$	$\bar{\gamma}$	\bar{r}
Western Europe	English	0.274	-199.503	28.491	0.057	-182.275	24.297	0.120
	French	0.363	-168.266	17.236	0.253			
	Italian	0.391	-162.113	12.163	0.071			
	German	0.415	-66.471	13.363	0.086			
	Dutch	0.437	-275.000	17.500	0.075			
	Portuguese	0.527	-275.000	22.500	0.325			
	Esperanto	0.538	-186.561	43.770	0.054			
	Spanish	0.585	-275.000	47.500	0.075			
Eastern Europe	Catalan	0.785	-32.559	16.153	0.092	-114.62	25.188	0.249
	Ukrainian	0.381	-160.021	12.882	0.225			
	Greek	0.390	-155.085	17.148	0.122			
	Russian	0.417	-80.443	44.299	0.485			
	Hungarian	0.428	-275.000	17.500	0.325			
Northern Europe	Czech	0.602	45.326	39.733	0.267	-179.522	20.145	0.209
	Serbo-Croatian	0.709	-62.503	19.567	0.068			
	Swedish	0.411	-158.172	19.545	0.493			
	Finnish	0.446	-166.834	19.323	0.099			
Non Europe	Norwegian	0.522	-194.055	21.782	0.073	-179.522	22.389	0.191
	Danish	0.668	-199.027	19.930	0.171			
	Tagalog	0.318	-147.633	49.448	0.137			
	Arabic	0.348	-275.000	17.500	0.125			
	Persian	0.352	-161.536	14.402	0.058			
	Hindi	0.441	-173.580	29.827	0.071			
	Urdu	0.492	-87.499	20.466	0.441			
	Turkish	0.524	-275.000	22.500	0.075			
	Cebuano	0.578	-139.896	15.685	0.103			
Sinhala	0.689	-98.418	6.761	0.446				
Non Europe	Swahili	0.757	-21.647	9.797	0.275	-179.522	22.389	0.191
	Indonesian	0.802	-225.000	37.500	0.175			

Table 2: #BlackLivesMatter social movement – Results obtained by our optimization process using Twitter data. The best model parameters (μ^*, γ^*, r^*) estimated for each language and the corresponding fitting error are reported. The languages are grouped into geographic categories, within which their order is from lower to higher fitting error.

Language	Error (\downarrow)	Best parameters		
		μ^*	r^*	γ^*
Portuguese	0.079	-15.032	43.627	0.293
Danish	0.103	37.500	6.250	0.237
French	0.116	-143.229	4.654	0.483
Arabic	0.171	-187.500	6.250	0.262
English	0.171	-237.500	8.750	0.437
Polish	0.173	-129.998	7.813	0.444
Ukrainian	0.179	-105.263	1.971	0.419
Catalan	0.207	-148.104	13.975	0.408
Turkish	0.216	-96.103	29.010	0.211
Russian	0.216	-176.576	0.884	0.242
Italian	0.228	-112.500	3.750	0.337
Azerbaijani	0.238	79.507	4.224	0.442
German	0.242	-74.876	9.848	0.366
Mongolian	0.299	-112.500	8.750	0.337
Croatian	0.309	114.992	6.689	0.385
Indonesian	0.312	-135.514	8.841	0.393
Spanish	0.315	-89.986	8.145	0.396
Swedish	0.323	-181.669	10.826	0.333
Greek	0.325	76.365	3.818	0.376
Serbian	0.326	-180.659	10.313	0.165
Finnish	0.344	-115.637	12.734	0.080
Bulgarian	0.344	-167.765	37.055	0.062
Korean	0.354	-77.711	5.008	0.468
Dutch	0.358	40.817	46.633	0.014
Norwegian	0.365	-187.746	11.676	0.388
Slovenian	0.369	-155.508	13.774	0.411
Serbo-Croatian	0.377	-174.138	5.240	0.156
Hindi	0.383	-122.453	48.200	0.034
Latvian	0.390	-147.599	5.417	0.395
Romanian	0.404	-166.494	8.209	0.495
Cebuano	0.421	-87.263	11.141	0.270
Czech	0.426	-128.022	12.856	0.331
Hungarian	0.510	-101.473	13.044	0.172
Hebrew	0.524	111.431	9.977	0.409
Slovak	0.538	-287.500	11.250	0.212
Lithuanian	0.539	47.500	8.750	0.412
Macedonian	0.572	-133.952	19.893	0.245
Persian	0.716	-187.500	21.250	0.312

Table 3: Ukrainian flag emoji – Results obtained by our optimization process using Twitter data related to the first period of the war in Ukraine. The best model parameters (μ^* , γ^* , r^*) estimated for each language and the corresponding fitting error are reported. The languages are ordered from the lowest to the highest fitting error.

C Supplementary material

Limited polarization in signed networks

Using a signed network instead can give scope for polarization, as shown in [40]. However, radicalization stays limited, in the following sense:

Proposition 5. – Limited polarization. *Consider the DeGroot update rule over a signed, possibly time-dependent network,*

$$X_{i,t+1} = \sum_{j=1}^N w_{ji,t} X_{j,t}, \quad (33)$$

where $w_{ji,t} \in [-1, 1]$ and $\sum_{j=1}^N |w_{ji,t}| = 1$.

Then:

1. $\forall t, \max_{(i,j)} (X_{i,t} - X_{j,t}) \leq 2 \max_i |X_{i,0}|$
2. *Either* $\forall t, \max_i \{X_{i,t}\} \leq \max_i \{X_{i,0}\}$ *or* $\forall t, \min_i \{X_{i,t}\} \geq \min_i \{X_{i,0}\}$.

Thus, the polarization achieved is limited by the initial situation, and there is one side that cannot get more radical than it was initially.

Proof. Taking the absolute value of the update rule gives:

$$|X_{i,t+1}| = \left| \sum_{j=1}^N w_{ji,t} X_{j,t} \right| \leq \sum_{j=1}^N |w_{ji,t}| |X_{j,t}| \leq \max_i |X_{i,t}| \underbrace{\sum_{j=1}^N |w_{ji,t}|}_{=1}. \quad (34)$$

Thus, $\forall t, \max_i |X_{i,t+1}| \leq \max_i |X_{i,t}|$. Result follow naturally from this observation. \square

Steering mechanism drives the model's dynamics

In the following, we call as maximal (resp. minimal) opinion the maximum (resp. minimum) agents' opinion at the end of a trial, and denote it by X_{\max} (resp. X_{\min}). More formally:

$$X_{\max} = \max_i X_{i,\infty}, \quad (35)$$

$$X_{\min} = \min_i X_{i,\infty}. \quad (36)$$

In practice, we estimate these quantities empirically using sufficiently long simulations. The heatmaps in Fig. 5 show how the X_{\max} and X_{\min} opinions among agents vary as a function of the strength of the GSM (controlled by γ and μ) in two distinct cases. We observe that: for $\beta = 0.05$ both the minimum and the maximum opinions decrease, while for $\beta = 0.95$ both increase. Previously, we identified such a behavior for the *average* opinion, however the generalization to the nodes' opinions was not obvious: increasing the steering mechanism, in particular for $\beta > \frac{1}{2}$, could have implied an increasing maximum and a decreasing minimum (since the negative reaction of negative reacting nodes is fueled by the behavior of positively reacting nodes). This suggests a specific interaction between the steering and propagation mechanisms: the propagation mechanism spreads those dynamics impulsed by the steering mechanism to the majority, towards the rest of the population. This highlights how the steering mechanism together with the propagation mechanism drive the dynamics of our model.

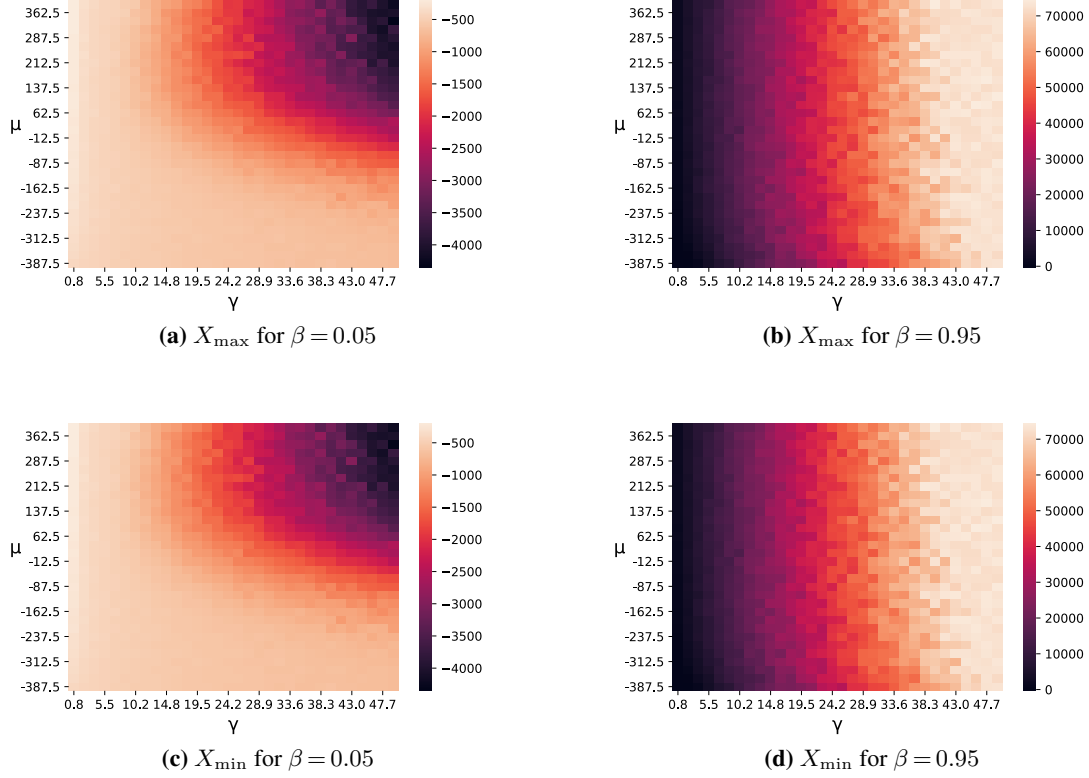


Figure 5: Effect of μ and γ on extreme opinions (maximal and minimal, X_{\max} , X_{\min}) recorded at the end of sufficiently long simulations. Two scenarios are examined: $\beta = \{0.05, 0.95\}$.

The SBM setting

For the plots we present in Sec. 4.2 we used the stochastic block model (SBM) to generate synthetic networks with two clusters of fixed sizes, c_1, c_2 , and fixed $\beta^{(1)}, \beta^{(2)}$ such that $c_1\beta^{(1)} + c_2\beta^{(2)} < \frac{1}{2}$ to avoid exploding dynamics. Some of the interpretations given here rely on this point, in particular the one for the effect of r . While the choice of the specific values of other parameters can be regarded as somehow arbitrary, choosing an SBM with two clusters of opposite majority reaction to information, aims at modeling agents forming opinions inside two distinct, yet connected communities.

The ambiguous role of inter-cluster propagation mechanism

Here we have a deeper look into the implications of the inter-cluster propagation mechanism in the SBM setting, which is a special sort of propagation mechanism. Our SBM graphs are generated randomly and characterized by two parameters: ρ is the probability with which two nodes of the same cluster are connected, r is the probability with which two nodes of different clusters are connected. Thus, when r gets close to ρ the model gets close to a structure-less model with $\bar{\beta} = c_1\beta_1 + c_2\beta_2$. We refer to *increasing isolation* when r gets closer to 0 and ρ closer to 1, and we will be looking at the maximal and minimal opinions in two different cases: $\beta_1 = 0.958, \beta_2 = 0.041$ (so clearly $\bar{\beta} > \frac{1}{2}$, the steering mechanism is overall self-exciting), $\beta_2 = 0.958, \beta_1 = 0.041$ (so clearly $\bar{\beta} < \frac{1}{2}$, the steering mechanism is overall self-cooling).

Increasing isolation has the effect of radicalizing dynamics inside each cluster, so that their interaction becomes weaker *with respect to* the steering mechanism: this creates differentiated dynamics depending on which case we find ourselves in. In the first case (overall self-exciting, displayed in the top row of

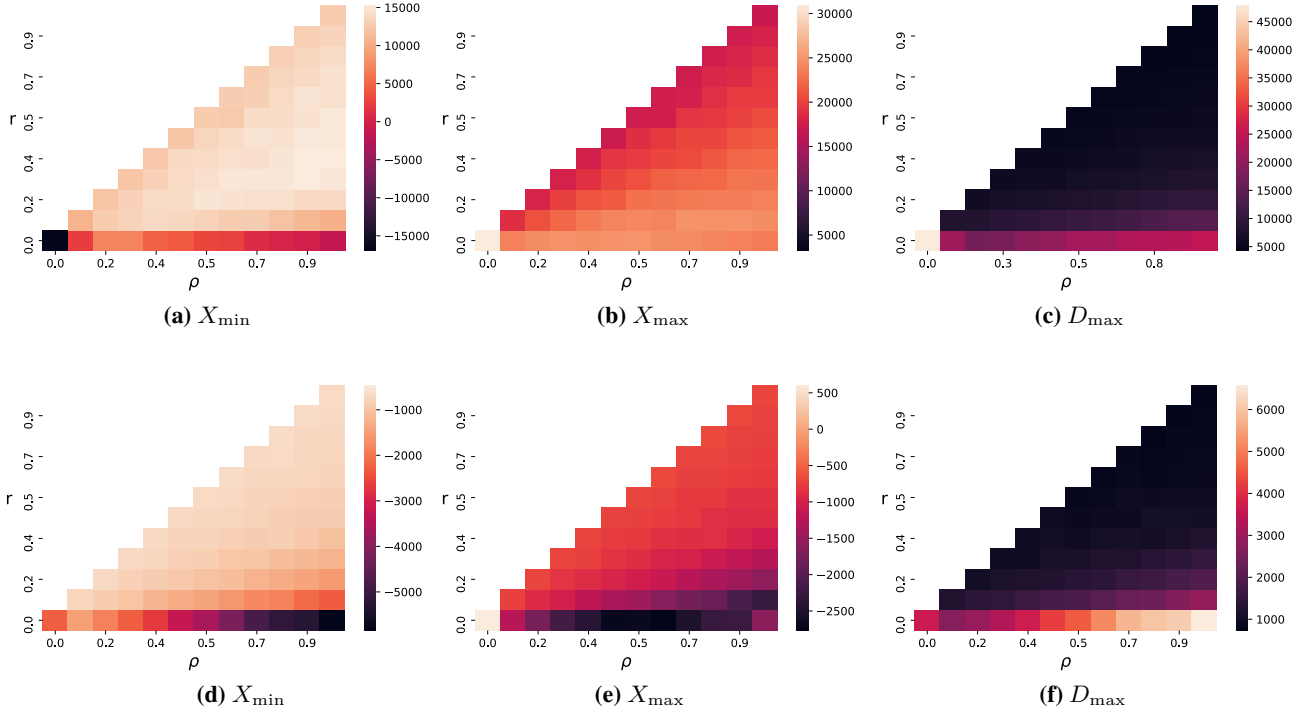


Figure 6: Heatmaps for the minimal and maximal opinions (X_{\min} , X_{\max}), as well as the maximal polarization (D_{\max} of Sec. 4.2) observed when using graphs generated by two SBM configurations. **Top row (a-c):** first case, SBM with $\beta^{(1)} = 0.958$, $\beta^{(2)} = 0.041$. **Bottom row (d-f):** second case, SBM with $\beta^{(1)} = 0.041$, $\beta^{(2)} = 0.958$.

Fig. 6), increasing isolation causes the dynamic in the majority cluster to be stronger, which in return feeds the dynamic of the minority one. As a consequence, maximal opinion increases whereas minimal opinion decreases. In the second case (overall self-cooling, displayed in the bottom row of Fig. 6), increasing isolation causes dynamics in the negatively-reacting majority cluster to get stronger, which decreases the minimal opinion but also decreases the strength of the steering mechanism. In return, this decreases the maximal opinion by calming the dynamics in the positively reacting minority cluster.

This is a good example of how complex the dynamics created by the interaction of steering mechanism and propagation mechanism (in particular inter-cluster propagation mechanism in an SBM setting) can get, while they are quite simple when considered by themselves.

Fitting method

Let us denote $S = \{S_t\}_{t \leq T}$ the time series from the data, and $m = \{m_t(\mu, \gamma, r)\}_{t \leq T}$ the time series issued by the model using a specific triplet of parameter values (μ, γ, r) . T is simply the length of the data time series, we will use model outcomes with the same observation length. Finding the best way to reproduce the data using the model can be formulated as follows:

$$(\mu^*, \gamma^*, r^*) = \arg \min_{(\mu, \gamma, r)} d(S, m(\mu, \gamma, r)), \quad (37)$$

where d is a scale-invariant distance (in a similar fashion as in [44]), so that

$$d(S, S') = \frac{\min_{\lambda} \sqrt{\sum_{t=1}^T (S_t - \lambda S'_t)^2}}{\|S\|}. \quad (38)$$

The optimal scaling coefficient is $\lambda^* = \frac{\langle S, S' \rangle}{\|S'\|}$. Given the stochastic nature of our model and the absence of analytic form for $\{m_t(\mu, \gamma, r)\}_{t \leq T}$, there is no way for us to use gradient-based optimization method, so that we will primarily rely on simulated annealing [45] for the fitting. As our model is stochastic, and we use a scale-free distance, it is likely that in noisy regions of the parameter space the model generates similar time series as the data without being informative. To cope with this issue, we add a variance indicator to the distance in order to avoid too noisy regions.

Our optimization process takes place in the parameter space $\Omega = [\underline{\mu}, \bar{\mu}] \times [\underline{\gamma}, \bar{\gamma}] \times [\underline{r}, \bar{r}]$, with bounds $\underline{\mu} = -500$, $\bar{\mu} = 500$, $\underline{\gamma} = 0$, $\bar{\gamma} = 50$, $\underline{r} = 0$, $\bar{r} = \frac{1}{2}$. The strategy we follow uses a first exploration phase, during which we get the model's fitting error to the data as well as an estimation of its variance at the center of each cell of the parameter grid, and then run K instances of simulated annealing using the K best points (i.e. solutions: triplets of parameter values) found earlier as initialization points. The simulated annealing requires us to define a neighborhood for any point of the parameter space. For a point x , we define its neighborhood $\mathcal{N}(x)$ as a cuboid centered at x , and of volume $vol < 1$ times the total volume of the space Ω . We also opt for a continuously decreasing temperature such that $\forall t, \text{temp}_t = \eta \text{temp}_{t-1}$. We set the hyperparameters at $T_0 = 10$, $\eta = 0.95$, $vol = 0.001$. A visual example of model fittings is shown in Fig. 7.

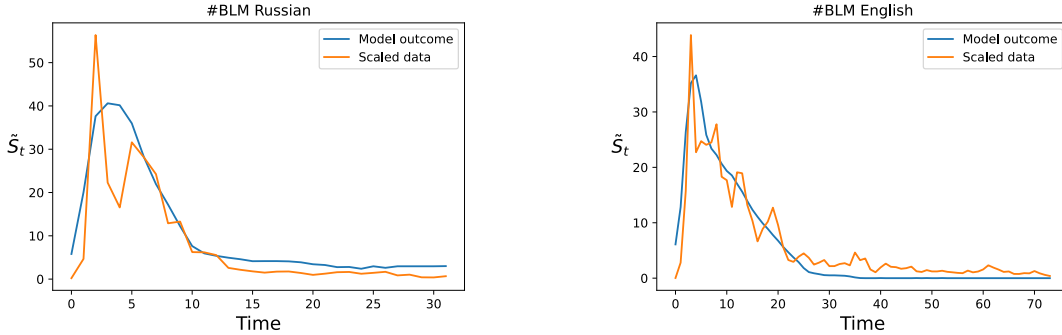


Figure 7: Two examples of fitted models and scaled data, for the spread of the Black Lives Matter (#BLM) hashtag in Russian and English tweets.

Model identifiability

When it comes to the outcome of the optimization process, that is the learned parameter values, an important point we discuss here is the *model identifiability*. More specifically, we would like to empirically verify in each use-case that the combination of parameter values (i.e. specific (μ, γ, r) triplets) that lead to good fitting of our model to the data lie in a relatively compact region of the parameter space (as opposed to being arbitrarily scattered therein, which would mean that multiple largely different parametrizations lead to equally good local optima). It is convenient to denote by $P^*(q)$ the top- q parametrizations, as to be the top q -quantile of triplets leading to the lowest data fitting error, where $q \in [0, 1]$ is a chosen threshold. Similarly we denote by $P(q)$ the denote a bootstrap subset of same size, containing randomly drawn triplets.

The main idea we employ aiming to investigate thoroughly model identifiability, is the comparison of these two sets, $P^*(q)$ and $P(q)$, in terms of a notion of variance, which we express as $\text{Variance}(P(q)) = \frac{1}{|P(q)|} \sum_{p \in P(q)} \|p - \bar{p}(q)\|_2$, where $\bar{p}(q)$ is the barycenter of $P(q)$ (similarly we compute for $P^*(q)$). Then, the procedure we follow is detailed below:

1. We first explore the parameter space by computing the fitting error of our model in each cell of a sufficiently fine-grained grid over Ω . Let the number of cells be denoted by $|\Omega|_{\text{grid}}$.
2. We let q vary in $[10^{-4}, 10^{-2}]$, and for each specific q value:

- 2a. we compile $P^*(q)$ with the $\lfloor q|\Omega|_{\text{grid}} \rfloor$ best triplets leading to the best model fitting;
- 2b. we compile multiple $P_i(q)$, $i = 1, \dots, B$ by drawing each time the same number of triplets, but selected uniformly at random. We set the number of bootstrap samples at $B = 10$.
3. We use the following metric:

$$\chi(q) = \frac{1}{B} \sum_i^B \left(\text{Variance}(P_i(q)) - \text{Variance}(P^*(q)) \right). \quad (39)$$

This measures the statistical significance of the concentration (i.e. low variance) of the best triplets in the parameter space, compared to bootstrap subsets of triplets. $\chi(q)$ is expected to give a high positive value when the top performing triplets are concentrated, and a smaller positive or even negative value when there is no statistical evidence for concentration.

The results of Fig. 8 show that $\chi(q)$ (y-axis) is always decreasing in q (x-axis) for the vast majority of cases (only 2 exceptions out of 41 languages). This general decreasing tendency of $\chi(q)$ indicates that the good performing triplets of parameter values lie at a relatively compact and delimited region of the parameter space, which indeed provides evidence for model identifiability.

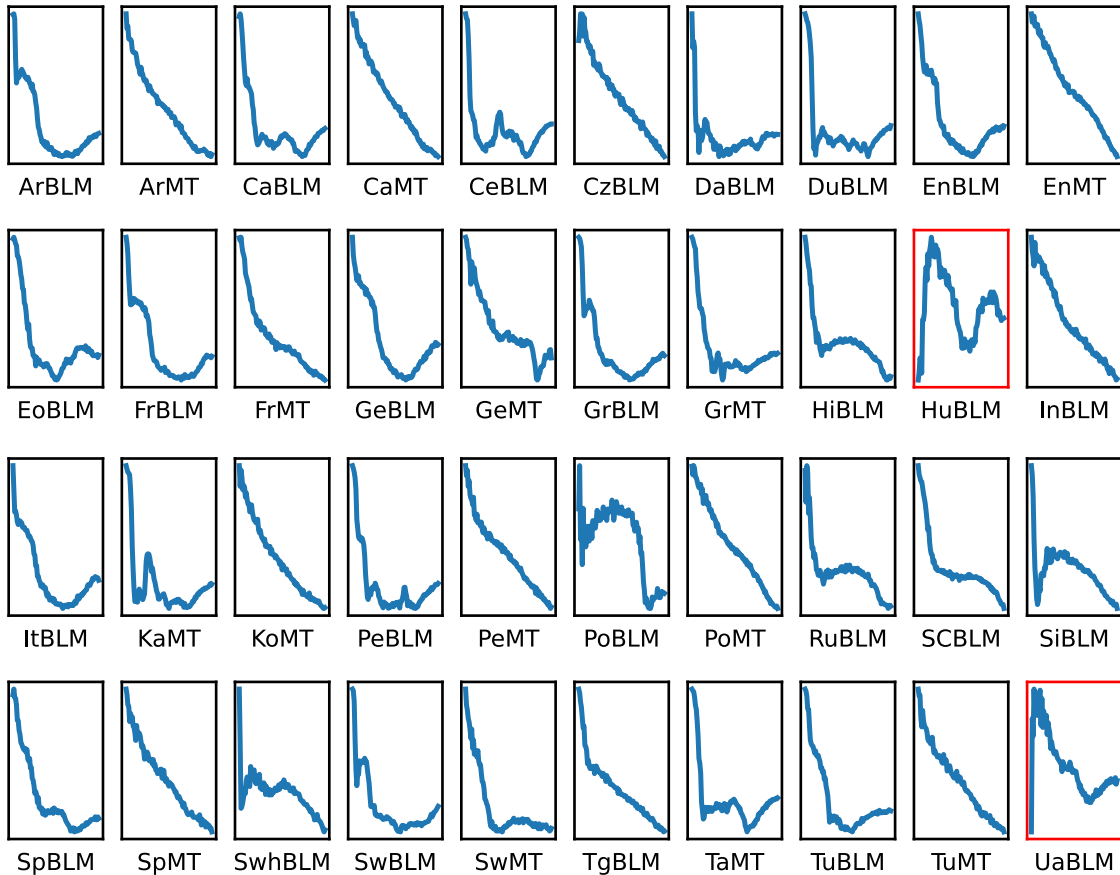


Figure 8: The bootstrap metric $\chi(q)$ (y-axis) as a function of q (x-axis) for each language. The metric decreases rapidly (with two exceptions indicated by red frames: HuBLM and UaBLM) as q increases and a wider q -quantiles of model parametrizations are included in the top performing set $P^*(q)$. This which provides evidence for the extend of our model’s identifiability in these scenarios.

References

- [1] M. Hilbert and P. López. The world’s technological capacity to store, communicate, and compute information. *science*, 332(6025):60–65, 2011.
- [2] P. Lorenz-Spreen, B.M. Mønsted, P. Hövel, and S. Lehmann. Accelerating dynamics of collective attention. *Nature communications*, 10(1):1–9, 2019.
- [3] Schroeder J. Lieberman A. Two social lives: How differences between online and offline interaction influence social outcomes. *Current Opinion in Psychology*, 31:16–21, 2020.
- [4] S. Boulianne. Twenty years of digital media effects on civic and political participation. *Communication research*, 47(7):947–966, 2020.
- [5] L. M.A. Bettencourt, A. Cintrón-Arias, D.I. Kaiser, and C. Castillo-Chávez. The power of a good idea: Quantitative modeling of the spread of ideas from epidemiological models. *Physica A: Statistical Mechanics and its Applications*, 2006.
- [6] F. Jin, E. Dougherty, P. Saraf, P. Mi, Y. Cao, and N. Ramakrishnan. Epidemiological modeling of news and rumors on Twitter. In *Proceedings of the 7th Workshop on Social Network Mining and Analysis (SNA-KDD)*, 2013.
- [7] M. Del Vicario, A. Bessi, F. Zollo, F. Petroni, A. Scala, G. Caldarelli, H.E. Stanley, and W. Quattrociocchi. The spreading of misinformation online. *Proceedings of the National Academy of Sciences*, 113(3):554–559, 2016.
- [8] Argyris Kalogeratos, Kevin Scaman, Luca Corinzia, and Nicolas Vayatis. Information diffusion and rumor spreading. In Petar M. Djurić and Cédric Richard, editors, *Cooperative and Graph Signal Processing*, pages 651–678. Academic Press, 2018.
- [9] A. Flache, M. Mäs, T. Feliciani, E. Chattoe-Brown, G. Deffuant, S. Huet, and J. Lorenz. Models of social influence: Towards the next frontiers. *Journal of Artificial Societies and Social Simulation*, (20), 2017.
- [10] F. Baumann, P. Lorenz-Spreen, I.M. Sokolov, and M. Starnini. Modeling echo chambers and polarization dynamics in social networks. *Physical Review Letters*, 124(4):048301, 2020.
- [11] Fabian Baumann, Philipp Lorenz-Spreen, Igor M. Sokolov, and Michele Starnini. Emergence of polarized ideological opinions in multidimensional topic spaces. *Phys. Rev. X*, 11:011012, 2021.
- [12] Walter Quattrociocchi, Guido Caldarelli, and Antonio Scala. Opinion dynamics on interacting networks: media competition and social influence. *Scientific reports*, 4(1):1–7, 2014.
- [13] M.H. DeGroot. Reaching a consensus. *Journal of the American Statistical Association*, 69(345):118–121, 1974.
- [14] N.E. Friedkin and E.C. Johnsen. Social influence networks and opinion change. *Advances in Group Processes*, 16:1–29, 1999.
- [15] Katz E. and Lazarsfeld P. *Personal influence; the part played by people in the flow of mass communications*. Free Press, Glencoe, 1955.
- [16] E. Bernays. *Crystallizing Public Opinion*. Boni and Liveright, New York, 1923.

- [17] E.S. Herman and N. Chomsky. *Manufacturing consent: The political economy of the mass media*. Random House, 2010.
- [18] R. Nadeau, E. Cloutier, and J-H. Guay. New evidence about the existence of a bandwagon effect in the opinion formation process. *International Political Science Review*, 14(2):203–213, 1993.
- [19] I. McAllister and T. S. Donley. Bandwagon, underdog, or projection? opinion polls and electoral choice in Britain, 1979-1987. *The Journal of Politics*, 53(3):720–741, 1991.
- [20] Y. Tsfati, H.G. Boomgaarden, J. Strömbäck, R. Vliegenthart, A. Damstra, and E. Lindgren. Causes and consequences of mainstream media dissemination of fake news: literature review and synthesis. *Annals of the International Communication Association*, 44(2):157–173, 2020.
- [21] J.R.P. Jr French. A formal theory of social power. *Psychological Review*, 63(3):181, 1956.
- [22] N.E. Friedkin and E.C. Johnsen. Social influence and opinions. *Journal of Mathematical Sociology*, 15(3-4):193–206, 1990.
- [23] R. Hegselmann and U. Krause. Opinion dynamics and bounded confidence models, analysis, and simulation. *Journal of Artificial Societies and Social Simulation*, 5(3), 2002.
- [24] R. Hegselmann and U. Krause. Opinion dynamics driven by various ways of averaging. *Computational Economics*, 25:381–405, 2005.
- [25] N.E. Friedkin. A formal theory of social power. *Journal of Mathematical Sociology*, 12(2):103–126, 1986.
- [26] P.D. Manrique, M. Zheng, Z. Cao, E. M. Restrepo, and N. F Johnson. Generalized gelation theory describes onset of online extremist support. *Physical review letters*, 121(4):048301, 2018.
- [27] Javad Ghaderi and R. Srikant. Opinion dynamics in social networks: A local interaction game with stubborn agents. *Proceedings of the American Control Conference*, 08 2012.
- [28] M. Granovetter. Threshold models of collective behavior. *American Journal of Sociology*, 83(6):1420, 1978.
- [29] S. Morris. Contagion. *The Review of Economic Studies*, 67(1):57–78, 2000.
- [30] K. Sznajd-Weron and J. Sznajd. Opinion evolution in closed community. *Int. J. Mod. Phys. C*, 11:1157–1166, 2000.
- [31] A. Grabowski and R.A. Kosinski. Ising-based model of opinion formation in a complex network of interpersonal interactions. *Physica A: Statistical Mechanics and its Applications*, 361(2):651–664, 2006.
- [32] Duncan J. Watts. A simple model of global cascades on random networks. *Proceedings of the National Academy of Sciences*, 99(9):5766–5771, 2002.
- [33] B. Golub and M.O. Jackson. Naïve learning in social networks and the wisdom of crowds. *American Economic Journal: Microeconomics*, 2(1):112–149, 2010.
- [34] R. Axelrod. The dissemination of culture. *Journal of conflict resolution*, 41(2):203–226, 1997.
- [35] G. Deffuant, D. Neau, F. Amblard, and G. Weisbuch. Mixing beliefs among interacting agents. *Advances in Complex Systems*, 3:87–98, 2000.

- [36] C. Schulze. Sznajd opinion dynamics with global and local neighborhood. *International Journal of Modern Physics C*, 15(06):867–872, 2004.
- [37] Shelley Boulianne. Social media use and participation: a meta-analysis of current research. *Information, Communication & Society*, 18(5):524–538, 2015.
- [38] Shelley Boulianne. Does internet use affect engagement? a meta-analysis of research. *Political communication*, 26(2):193–211, 2009.
- [39] D. Acemoglu, G. Como, F. Fagnani, and A. Ozdaglar. Opinion fluctuations and disagreement in social networks. *Mathematics of Operations Research*, 38:1–27, 2013.
- [40] Linh Thi Hoai Nguyen, Takayuki Wada, Izumi Masubuchi, Toru Asai, and Yasumasa Fujisaki. Opinion formation over signed gossip networks. *SICE Journal of Control, Measurement, and System Integration*, 10(3):266–273, 2017.
- [41] Emmanuel Abbe. Community detection and stochastic block models: Recent developments. *Journal of Machine Learning Research*, 18(177):1–86, 2018.
- [42] T. Alshaabi, J.L. Adams, M.V. Arnold, J.R. Minot, D.R. Dewhurst, A.J. Reagan, C.M. Danforth, and P.S. Dodds. Storywrangler: A massive exploratorium for sociolinguistic, cultural, socioeconomic, and political timelines using twitter. *Science Advances*, 7(29):eabe6534, 2021.
- [43] Noé Gaumont, Maziyar Panahi, and David Chavalarias. Reconstruction of the socio-semantic dynamics of political activist Twitter networks — Method and application to the 2017 French presidential election. *Plos one*, 13(9):e0201879, 2018.
- [44] Jaewon Yang and Jure Leskovec. Patterns of temporal variation in online media. In *Proceedings of the ACM International Conference on Web Search and Data Mining*, pages 177–186, 2011.
- [45] Scott Kirkpatrick, C Daniel Gelatt, and Mario P Vecchi. Optimization by simulated annealing. *Science*, 220(4598):671–680, 1983.